Contact Engineering of Monolayer CVD MoS₂ Transistors

Abdullah Alharbi and Davood Shahrjerdi

Electrical and Computer Engineering, New York University, Brooklyn, NY, 11201 Email: <u>davood@nyu.edu</u>

Introduction: Transition metal dichalcogenides (TMDs) are promising for next-generation electronic and optoelectronic device applications. However, the development of a viable TMD device technology requires an effective strategy for making low-resistance contacts to these materials. In addition, large-area synthesis of low-defect TMD crystals is essential for transforming basic device studies into commercial products. Here, we show large-area synthesis of monolayer (ML) MoS₂ using chemical vapor deposition (CVD) with electron mobility of ~64cm²/V.s at room temperature. We performed contact engineering through a combination of work function engineering and effective n-type doping of MoS₂ using engineered sub-stoichiometric HfO_x. Our results indicate significant reduction of the contact resistance to ~480Ω.μm without degrading key transistor properties such as subthreshold swing (~125mV/dec), mobility (~64cm²/V.s), and I_{ON}/I_{OFF} ratio (>10⁶).

Experiment and Results: We fabricated top-gated transistors from ML-MoS₂ grown by CVD. Fig. 1 shows the device fabrication flow. The ML-MoS₂ films were grown from MoO₃ and sulfur solid precursors at 850°C. The resulting CVD MoS₂ flakes are generally in excess of 150 μ m (Fig.2). Raman and photoluminescence (PL) measurements confirmed the monolayer thickness. Fig. 3 schematically illustrates the structure of our top-gated four-point transistors. First, we studied the effect of the metal electrode choice (Ti and Ag) on the contact resistance. Despite the nearly similar work functions of Ti and Ag (Φ_{Ti} =4.33eV, Φ_{Ag} =4.26eV), their resulting Schottky barrier height (SBH) with ML-MoS₂ (and thus their contact resistance) is noticeably different from one another (Fig. 4). Although work function engineering is effective in reducing the contact resistance, it appears to be inadequate because Fermi level pinning at the metal/MoS₂ interface governs SBH.

In Schottky-type transistors, increasing the semiconductor doping is an effective strategy for promoting the tunneling of charge carriers into the channel, thereby reducing the contact resistance (Fig. 5). The use of substoichiometric metal oxides (e.g. HfO_x, TiO_x, etc) has shown to induce n-type doping in MoS₂^{1, 2}. Despite these encouraging reports on the significant reduction of the contact resistance, the transistors suffer from noticeable degradation of the subthreshold swing and I_{ON}/I_{OFF} ratio. However, considering the air stability of this method and its compatibility with CMOS processes, we examined the utility of sub-stoichiometric HfO_x films for reducing the contact resistance of our devices. The composition of the HfO_x film was adjusted by varying its deposition conditions during the atomic layer deposition at 200°C. To qualitatively evaluate the effect of different HfO_x films on the n-type doping level of the CVD ML-MoS₂, we monitored the evolution of the PL and Raman spectra. Fig. 6 shows the representative PL and Raman spectra for three ML-MoS₂ flakes capped with no HfO_x, with HfO_x inducing low doping (LD), and with HfO_x inducing high doping (HD). The Raman data clearly shows the shift in the position of the E_{2g} Raman peak and its amplitude, as well as the position of the PL peak with varying the doping level. Next, we examined the transfer and output characteristics of the LD and HD top-gated MoS2 transistors with Ti (Fig. 7) and Ag (Fig. 8) electrodes. The data indicate significant improvement of the ON current for both Ti and Ag electrodes due to the n-type doping by HfO_x. Unlike the transistors with Ti electrodes, we observe that the subthreshold swing and the I_{ON}/I_{OFF} ratio of the transistors with Ag electrodes remain unchanged. We surmise that the observed behavior might be due to the local oxidation of the Ti electrodes near the channel region. Fig. 9a shows the transmission line measurements (TLM) of an HD MoS₂ transistor with Ag electrode, showing a contact resistance of \sim 480 Ω ,µm. Fig. 9b shows the summary of the contact resistance for LD and HD MoS₂ transistors with Ti and Ag contacts. Finally, we studied the effect of the n-type doping by HfO_x on the mobility of the electron carriers. The intrinsic mobility was calculated from the slope of the four-point conductance (G_{4nt}) and the measured capacitance-voltage characteristics of the transistors (not shown). The devices exhibit relatively high electron mobility ranging from ~47 to 64cm²/V.s. at room temperature. Fig. 10 shows the variation of the intrinsic mobility for HD MoS₂ devices with temperature. The mobility variation at temperatures above 100°K follows a power-law dependence, indicating the dominance of the acoustic phonon scattering.

Conclusion: We demonstrated significant reduction of the contact resistance (to $\sim 480\Omega.\mu m$) for tope-gated monolayer CVD MoS₂ through a combination of work function engineering and effective n-type doping by HfO_x. In addition to improving the contact resistance, our approach maintains the mobility ($\sim 64 cm^2/V.s.$), I_{ON}/I_{OFF} ratio ($>10^6$), and subthreshold swing ($\sim 125 mV/dec$) of these transistors.

This research was supported by NSF-1638598 and used resources of the Center for Functional Nanomaterials, which is a U.S. DOE Office of Science Facility, at Brookhaven National Laboratory under Contract No. DE-SC0012704.

[1] A. Rai et al., Nano Lett., vol. 15, p. 4329, (2015).

[2] A. Sanne et al., Nano Lett., vol. 15, p. 5039, (2015).

CVD growth of MoS₂ on p+ Si substarte with 285nm SiO₂

Define device active area (EBL and CF₄/O₂ RIE)

Form source/drain metal contact (Ag or Ti)/Au

Atomic layer deposition of HfO_x (adjust MoS₂ doping level)

Top gate electrode (EBL and Cr/Au deposition)

Fig. 1: Top-gated ML-MoS, device fabrication process.



Fig. 2: Optical image of large monolayer MoS_2 flakes (scale bar $50\mu m$).

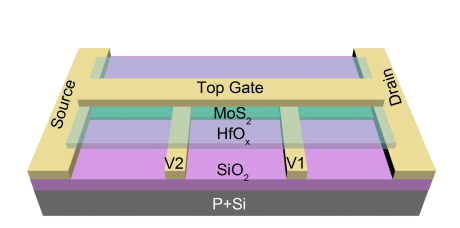


Fig. 3: Schematic illustration of a top-gated four-point ML-MOS, transistor.

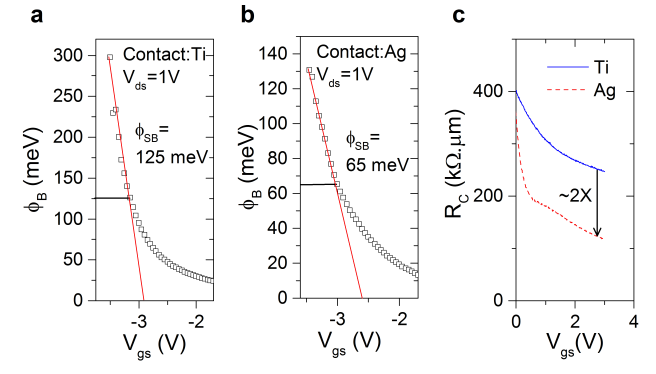
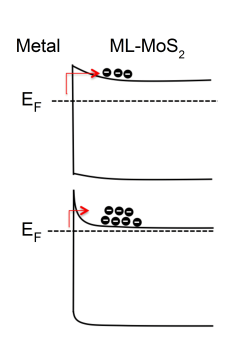
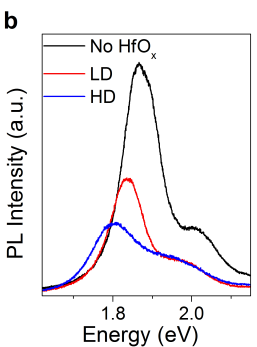


Fig. 4: Measured SBH of ML-MoS₂ transistors with (a) Ti, and (b) Ag electrodes. (c) Comparison of the specific contact resistance (R₂).



A No HfO_x A_{1g} LD HD A_{1g} A_{1g} Raman Shift (cm⁻¹)



bTi-LD

Ti-HD

Ti-HD

L=20 μm

(μπ/γ 10⁻³

10⁻⁷

10⁻⁷

V_{ds}=1V

V_{gs}(V)

V_{ds}(V)

Fig. 5: Effect of n-type doping on energy band structure and SBH.

Fig. 6: Evolution of (a) Raman, and (b) PL with varying n-type doping of ML-MoS₂.

Fig. 7: (a) Transfer, and (b) output characteristic of devices with Ti.

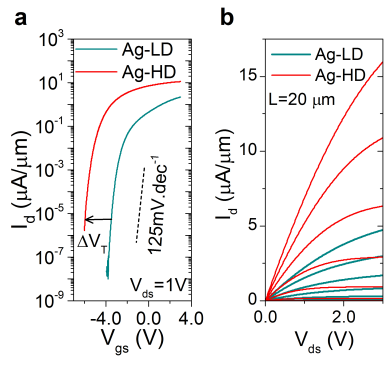


Fig. 8: (a) Transfer, and (b) output characteristics of devices with Ag.

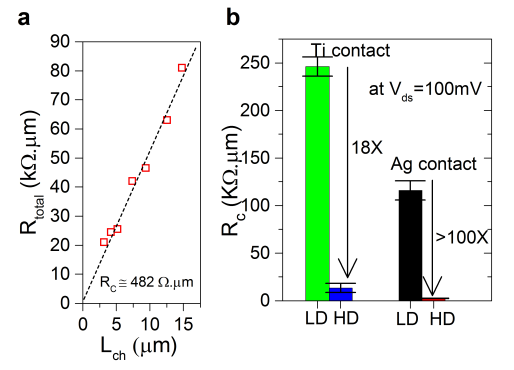


Fig. 9: (a) TLM measurements of HD-Ag device, (b) summary of contact resistance measurements.

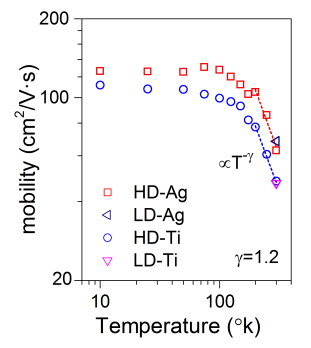


Fig. 10: Intrisinc mobility of ML-MoS₂ devices with different level of n-doping.